Cell Reports, Volume *39*

Supplemental information

Suppression of p53 response by targeting p53-Mediator binding with a stapled peptide

Benjamin L. Allen, Kim Quach, Taylor Jones, Cecilia B. Levandowski, Christopher C. Ebmeier, Jonathan D. Rubin, Timothy Read, Robin D. Dowell, Alanna Schepartz, and Dylan J. Taatjes

Supplemental Information

Suppression of p53 response by targeting p53-Mediator binding with a stapled peptide

Allen, BL[1‡]; Quach, K[2‡]; Jones, T[1‡]; Levandowski, CB[1]; Ebmeier, CC[1]; Rubin, JD[1]; Read, T[1,3]; Dowell, RD[4,5]; Schepartz, A[2,6,7]; Taatjes, DJ.[1*§]*

[1]Dept. of Biochemistry, University of Colorado, Boulder, CO, USA
[2]Dept. of Chemistry, Yale University, New Haven, CT, USA
[3]Dept. of Medicine, Division of Genetics, Brigham & Women's Hospital, Harvard Medical School, Boston, MA, USA
[4]Dept. of Molecular, Cellular, and Developmental Biology, University of Colorado, Boulder, CO, USA
[5]BioFrontiers Institute, University of Colorado, Boulder, CO, USA
[6]Dept. of Molecular, Cellular, and Developmental Biology, Yale University, New Haven, CT, USA
[7]Current address: Dept. of Chemistry, University of California, Berkeley, CA, USA

‡equal contribution
*corresponding authors
§Lead contact

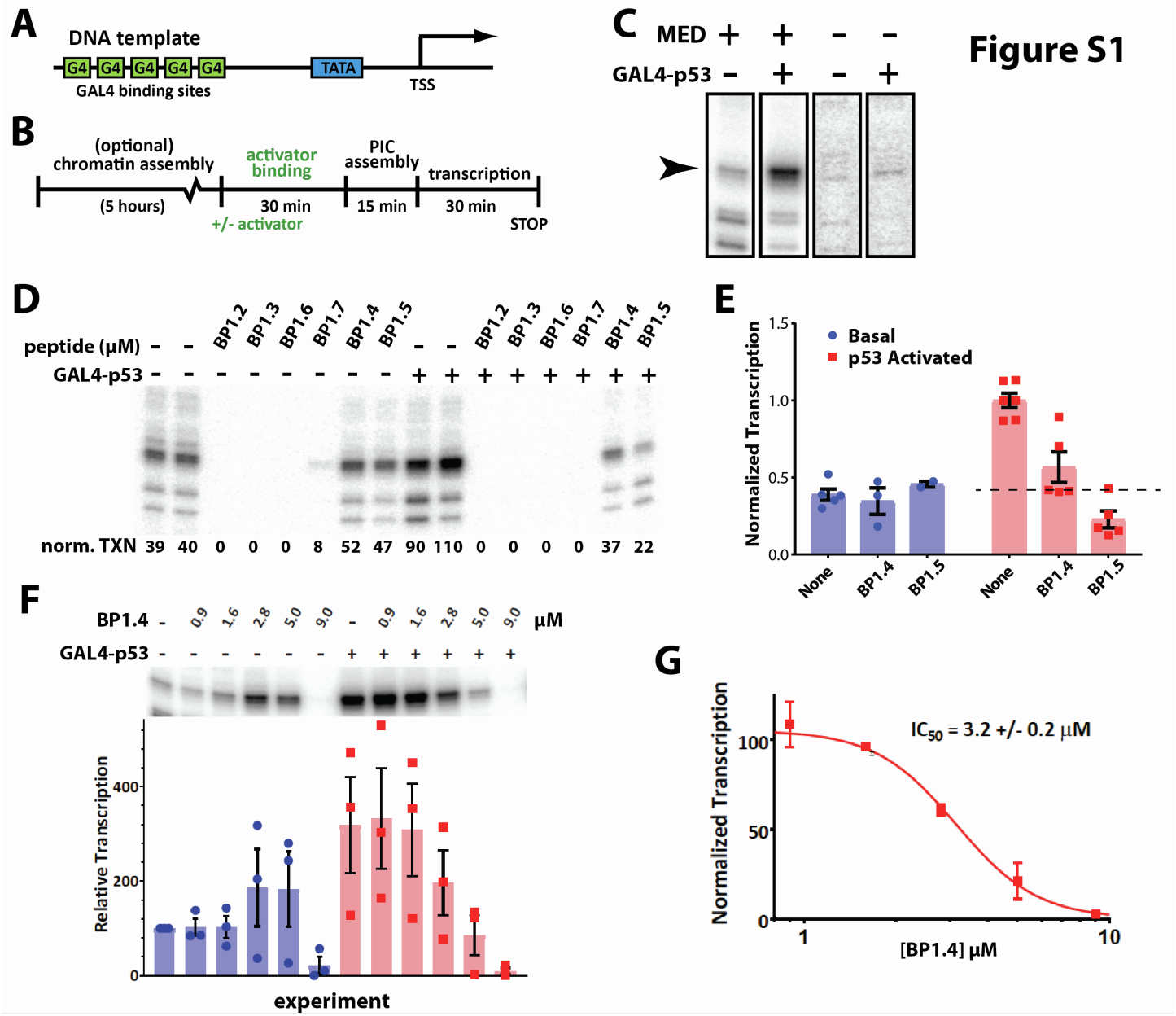

Figure S1. *In vitro* screening protocol; functional screening of stapled and unstapled p53AD1 mimics. Related to Figures 1 and 2. (A) Promoter DNA template scheme. (B) Overview of reconstituted *in vitro* transcription assay (chromatin assembly optional; PIC = Pre-Initiation Complex: TFIIA, TFIIB, TFIID, TFIIE, TFIIF, TFIIH, Mediator, and pol II). (C) Representative *in vitro* transcription data from naked DNA templates, showing p53- and Mediator-dependence. (D) Representative data (*in vitro* transcription) using each peptide at 5 μM concentration, in presence (+) or absence (–) of GAL4-p53. Note that only BP1.4 and BP1.5 show ability to inhibit p53-activated transcription while not markedly affecting basal transcription. (E) Scatter plot summarizing *in vitro* transcription data for BP1.4 and BP1.5 peptides in absence (basal) or presence (activated) of GAL4-p53. Dashed line represents basal transcription level. (F) Representative data (top) and scatter plot (bottom) summarizing results from titration experiments with BP1.4 peptide under basal (– GAL4-p53) or activated (+ GAL4-p53) conditions. (G) IC_{50} plot

summarizing inhibitory activity of BP1.4 peptide. For data panels (D-G), transcription was normalized to GAL4-p53 in absence of added peptide.

Figure S2

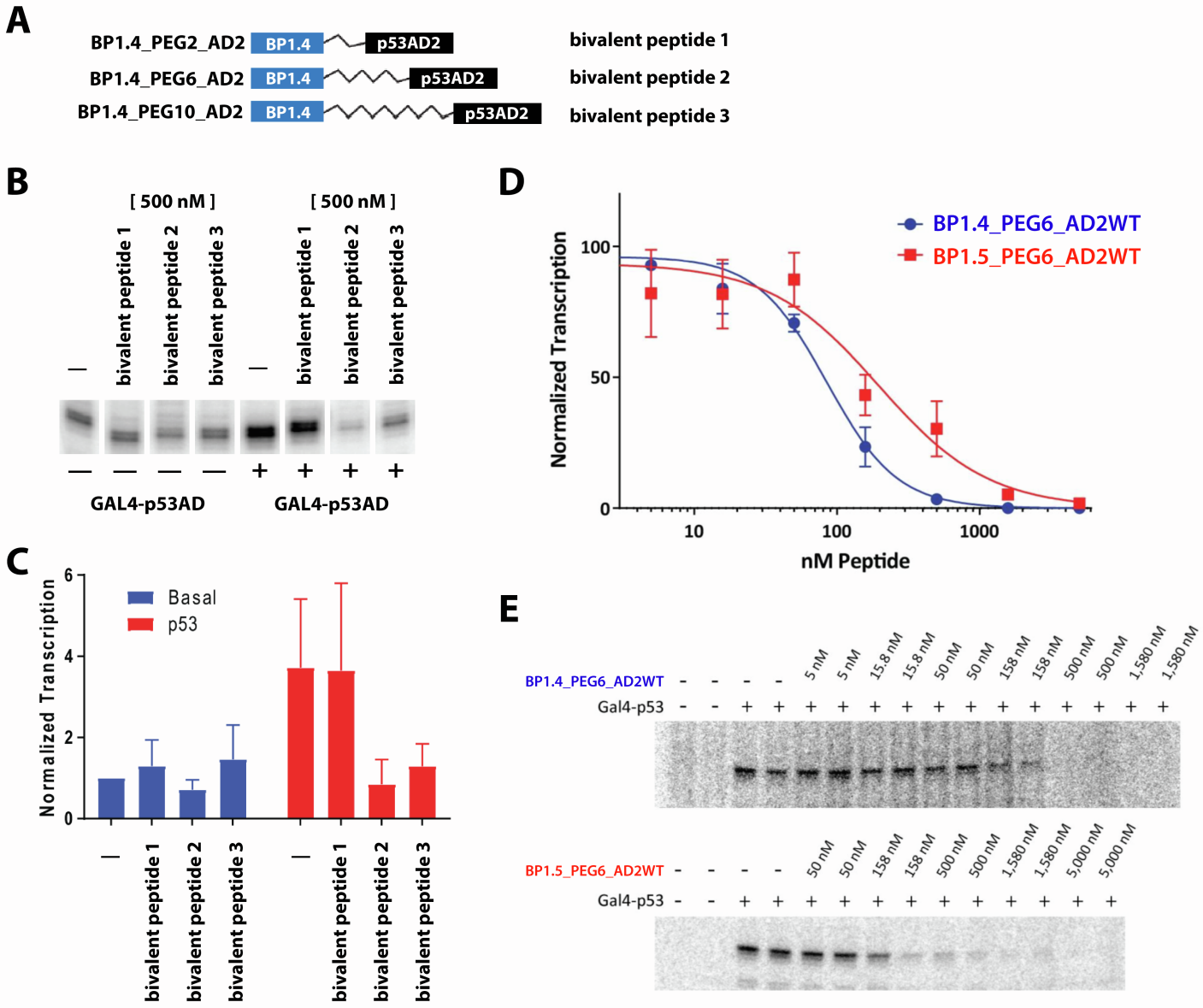

Figure S2. Testing different PEG linker lengths to tether BP1.4 (stapled p53AD1 mimic) to p53AD2 sequence. Related to Figure 2. (A) Schematic of 3 different PEG linkers to generate bivalent peptide 1, 2, or 3. (B) Representative *in vitro* transcription data and (C) bar plot summary (n = 4; bars = s.e.m.) of bivalent peptides with different PEG linker lengths. Note that a PEG6 or PEG10 linker showed enhanced ability to block p53-activated transcription, whereas PEG2 linker (i.e. bivalent peptide 1) did not. (D) IC_{50} plot showing activity of bivalent peptide (i.e. BP1.4_PEG6_AD2WT) vs. an AD1 derivative (BP1.5). Points with error bars represent standard error of the mean, with n = 3 to 8 (blue dots) or n = 3 to 4 (red squares). The IC_{50} value for BP1.5_PEG6_AD2WT was 200 ± 88nM whereas the IC_{50} for the bivalent peptide BP1.4_PEG6_AD2WT was 85 ± 11nM (see **Figure 2**). (E) Representative *in vitro* transcription data used for the plot in panel D.

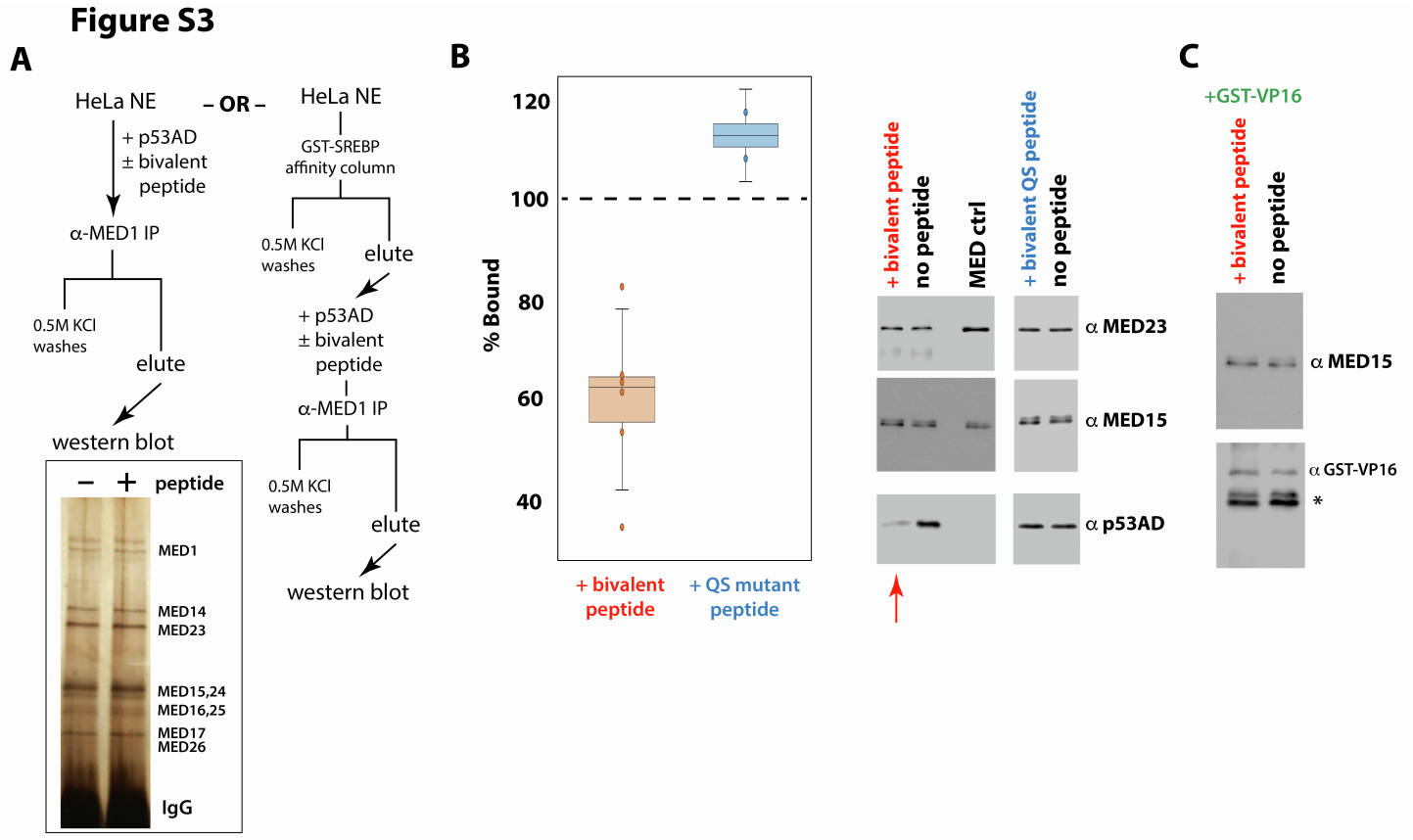

Figure S3. Bivalent peptide blocks p53AD-Mediator binding. Related to Figure 2. (A) Overview of binding assays used. A crude Mediator sample was isolated from HeLa NE with a GST-SREBP affinity column (Naar et al., 1999) prior to incubation with p53AD (2 μM) ± bivalent peptide (5 μM) in one of the protocols (right). Inset: silver-stained gel of the MED1 IP, showing a relatively pure Mediator sample. (B) Scatterplot (left) summarizing p53AD binding to Mediator in presence of bivalent peptide or a QS mutation in p53AD2. The percent binding is relative to p53AD bound to Mediator in absence of added peptide (dashed line); p53AD quantitation was normalized to total Mediator, as assessed by quantitation of MED15 signal (and/or MED1 in some cases; n = 4 biological and 6 total replicates). Representative data (western blot) shown at right. Simliar results were obtained with either protocol shown in panel A. (C) Binding assay shown at right in panel A was used to probe VP16-Mediator binding (n = 2), which revealed that VP16-Mediator binding is not inhibited by the bivalent peptide. Normalization of bound GST-VP16 to MED15 in fact showed a 1.67-fold increase in Mediator-bound VP16 in the +peptide experiments. Representative western blot shown. Asterisk: free GST.

Figure_S4

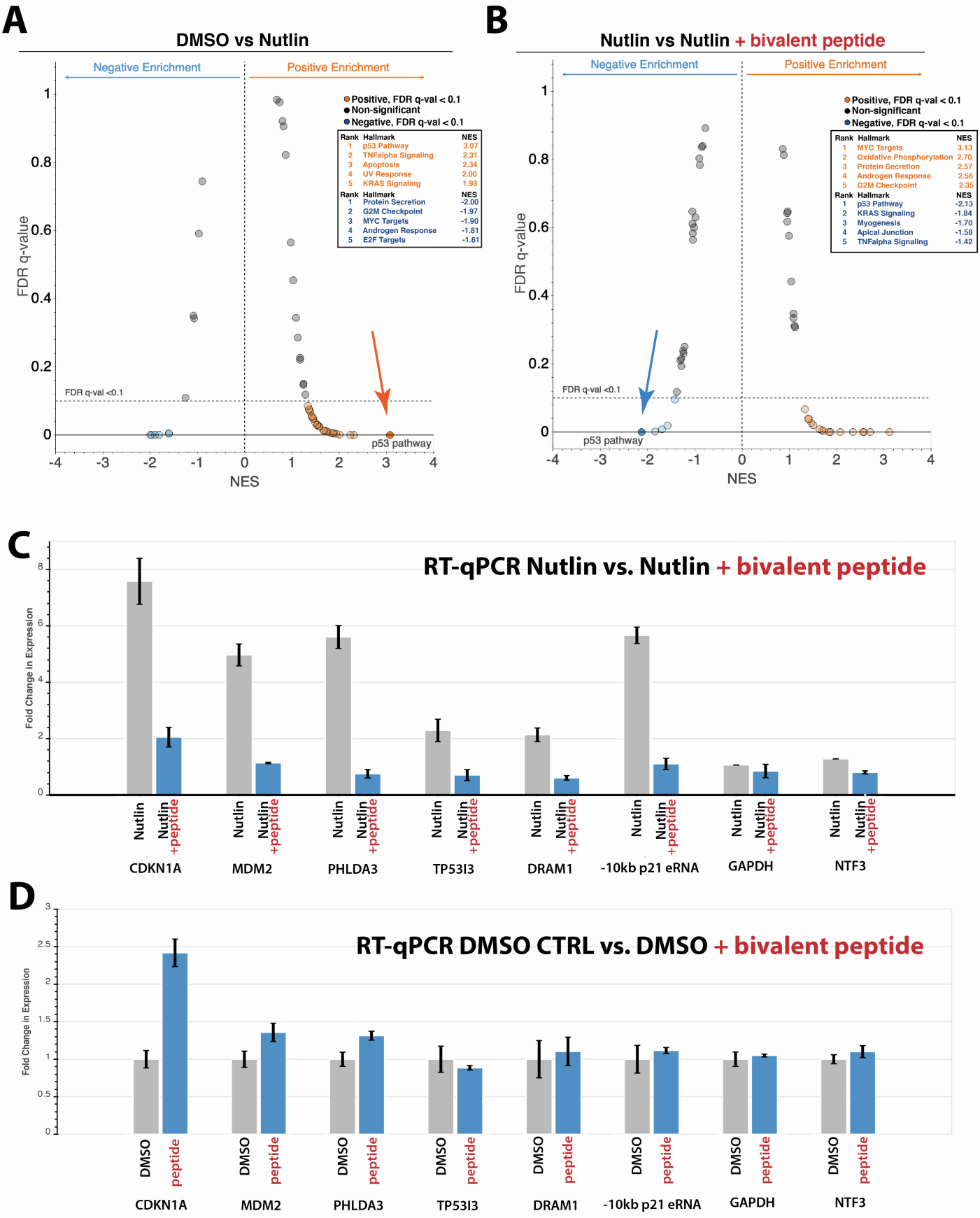
A
DMSO vs Nutlin
Negative Enrichment
Positive Enrichment
Positive, FDR q-val < 0.1
Non-significant
Negative, FDR q-val < 0.1
Rank Hallmark NES
1 p53 Pathway 3.07
2 TNFalpha Signaling 2.31
3 Apoptosis 2.34
4 UV Response 2.00
5 KRAS Signaling 1.93
Rank Hallmark NES
1 Protein Secretion -2.00
2 G2M Checkpoint -1.97
3 MYC Targets -1.90
4 Androgen Response -1.81
5 E2F Targets -1.61
FDR q-value
FDR q-val <0.1
p53 pathway
NES
B
Nutlin vs Nutlin + bivalent peptide
Negative Enrichment
Positive Enrichment
Positive, FDR q-val < 0.1
Non-significant
Negative, FDR q-val < 0.1
Rank Hallmark NES
1 MYC Targets 3.13
2 Oxidative Phosphorylation 2.70
3 Protein Secretion 2.57
4 Androgen Response 2.56
5 G2M Checkpoint 2.35
Rank Hallmark NES
1 p53 Pathway -2.13
2 KRAS Signaling -1.84
3 Myogenesis -1.70
4 Apical Junction -1.58
5 TNFalpha Signaling -1.42
FDR q-value
FDR q-val <0.1
p53 pathway
NES
C
RT-qPCR Nutlin vs. Nutlin + bivalent peptide
Fold Change in Expression
Nutlin
Nutlin +peptide
CDKN1A
MDM2
PHLDA3
TP53I3
DRAM1
-10kb p21 eRNA
GAPDH
NTF3
D
RT-qPCR DMSO CTRL vs. DMSO + bivalent peptide
Fold Change in Expression
DMSO
peptide
CDKN1A
MDM2
PHLDA3
TP53I3
DRAM1
-10kb p21 eRNA
GAPDH
NTF3

Figure S4. Additional RNA-seq results and supporting RT-qPCR data. Related to Figures 3 and 4. (A, B) GSEA moustache plots (RNA-seq experiment 1) that show (A) Nutlin treatment strongly induces p53 pathway activation (NES: 3.07), as expected, and that (B) in Nutlin-treated cells, the bivalent peptide inhibits p53 pathway activation (NES: –2.13). (C, D) RT-qPCR results are consistent with RNA-seq data and show suppression of p53 target gene expression by the bivalent peptide (C) or negligible effects in the absence of Nutlin-dependent p53 activation (D). Bars represent standard error of the mean (n = 2).

Figure_S5

A **B**

[RNA-seq experiment 2: analysis in serum-free media]

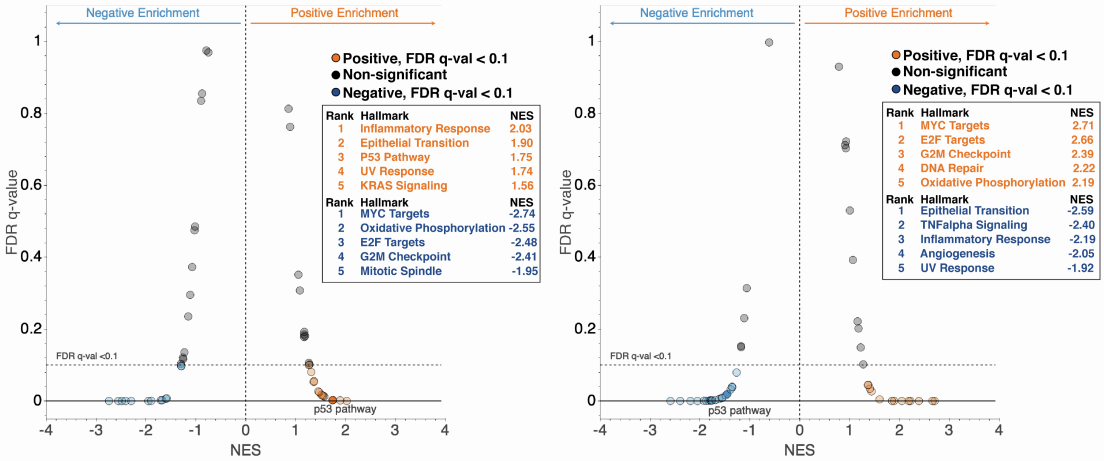

DMSO vs. Nutlin

Nutlin vs. Nutlin + peptide

C

Volcano plot

[RNA-seq experiment 2]

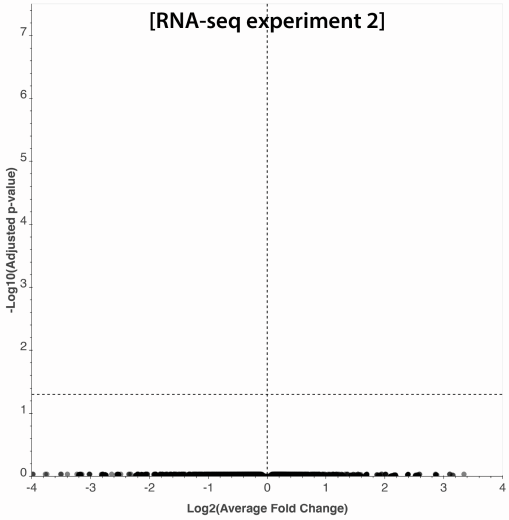

DMSO vs. DMSO + peptide

D

GSEA

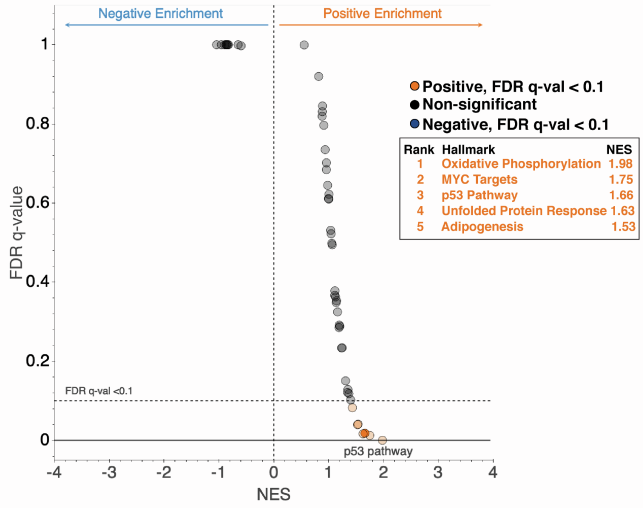

DMSO vs. DMSO + peptide

Figure S5. Bivalent peptide blocks p53 response in Nutlin-treated HCT116 cells, but causes no significant changes in pol II transcription in absence of p53 activation (RNA-Seq experiment 2); evidence for weak p53 activation in DMSO control + peptide experiments. Related to Figures 3 and 4. (A, B) GSEA moustache plots (RNA-seq experiment 2) show (A) Nutlin treatment induces p53 pathway activation (NES: 1.75), and that (B) in Nutlin-treated cells, the bivalent peptide inhibits p53 pathway activation (NES: –1.45). Note that RNA-seq experiment 2 (biological triplicate samples) differed from RNA-seq experiment 1 (biological replicate samples) in that serum-free media was used, based upon reports that it could enhance peptide uptake by cells (Brown et al., 2013; Chang et al., 2013). In retrospect, this likely ensured a weak Nutlin response due to p53 activation triggered by serum removal (Blagosklonny et al., 1997; Shi et al., 2012). Consistent with this notion, the p53 pathway activation was markedly reduced in Nutlin-treated cells (NES: 1.75) compared with experiment 1, with GSEA NES = 3.07 for p53 pathway in Nutlin-treated cells (**Figure S4A**). Despite these limitations, GSEA results from RNA-seq experiment 2 show suppression of p53 activation by the bivalent peptide. (C) Volcano plot showing that the bivalent peptide causes no significant changes in pol II transcription in the absence of p53 activation (RNA-seq experiment 2). These results are similar to RNA-seq experiment 1 (**Figure 3E**). (D) GSEA moustache plot (RNA-seq experiment 1) comparing DMSO control conditions ± bivalent peptide. Note a weak p53 pathway activation (NES=1.66) that is consistent with *in vitro* data (**Figure S1F**); in cells, the weak activation could reflect a modest disruption of p53-MDM2 interactions, but this remains to be rigorously tested.

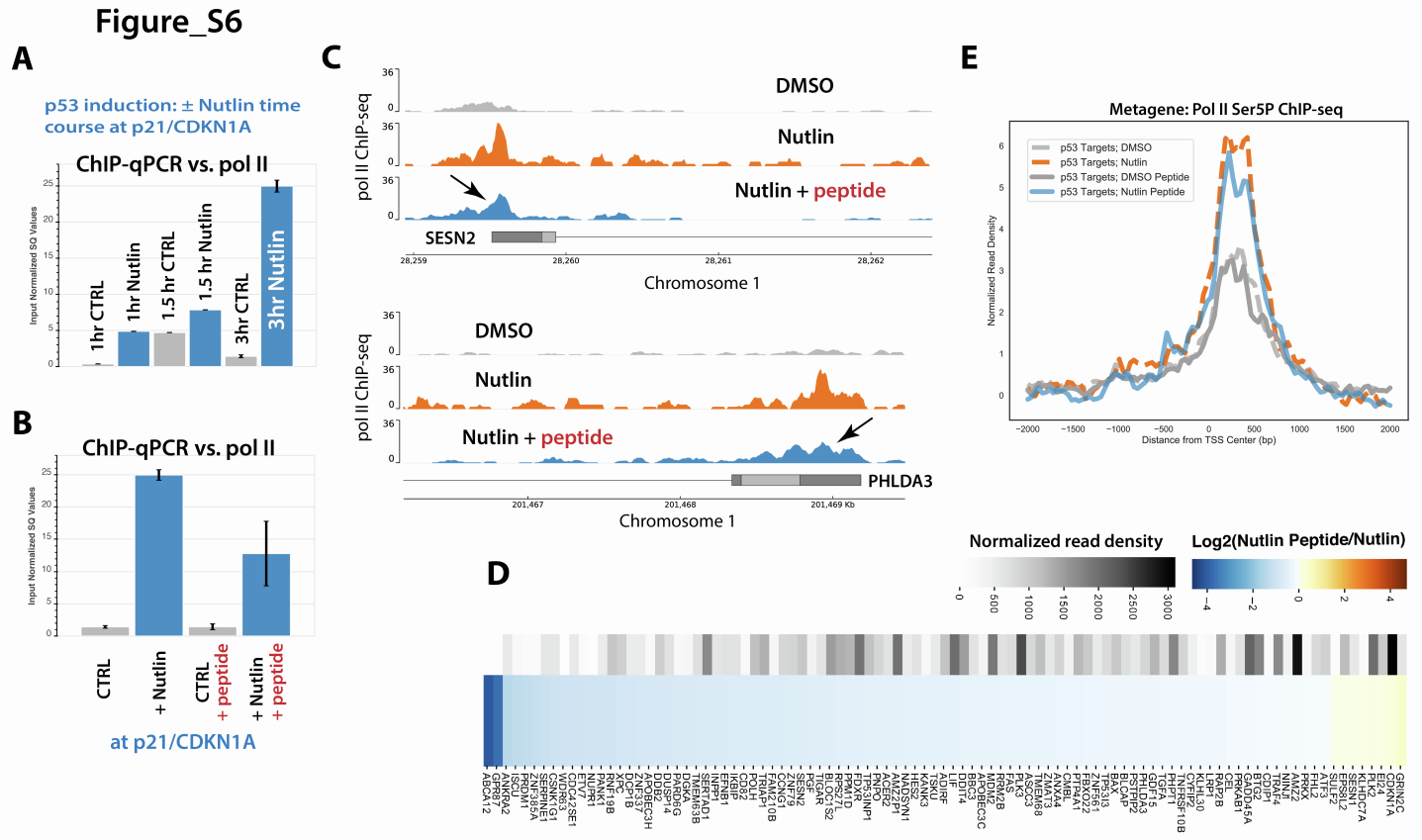

Figure S6. Summary of pol II CTD Ser5P ChIP-seq data; related to Figure 4. (A) Time-course ChIP-qPCR that provided the basis for a 3hr post-Nutlin time point for ChIP-seq experiments. This time point is identical to that used for RNA-seq. (B) ChIP-qPCR at the p21/CDKN1A locus, showing i) increased pol II occupancy in Nutlin-stimulated cells but ii) reduced pol II occupancy in cells treated with the bivalent peptide. (C) Example pol II CTD Ser5P ChIP-seq traces at p53 target gene promoters. Consistent with the RNA-seq data, pol II occupancy is increased in Nutlin-treated cells, but pol II occupancy is reduced in cells treated with the bivalent peptide. (D) Summary heatmap at core p53 target genes (Andrysik et al., 2017) showing overall reduced pol II occupancy at promoter regions (see Methods). The heatmap represents the log2(Nutlin+Peptide/Nutlin adjusted read counts) in which blue indicates a reduction of pol II occupancy in the Nutlin+peptide vs. Nutlin samples. The separate black-and-white heatmap represents the average Signal-to-Noise Ratio (SNR) normalized read counts, derived from the CHIPIN method (Polit et al., 2021). Promoters with higher read density will have darker shading. (E) Ser5P pol II ChIP-seq metagene at the TSSs of a subset of p53 target genes. Note that ChIP-seq provides data at a snap-shot in time, whereas RNA-seq represents cumulative effects over time. Thus, we observe two populations of responses at p53 target genes (Andrysik et al., 2017) as seen by ChIP-seq (t = 3hr) in which the adjusted read density in Nutlin+Peptide sample compared to Nutlin is either unchanged or higher (27 TSSs) or lower (70 TSSs). This probably reflects differential induction of p53 target genes at the t = 3hr time point and is also reflected in the heatmap in panel D.

The ChIP-seq metagene shown is derived from the set of 70 TSSs and shows that Nutlin + bivalent peptide has lower Ser5P pol II occupancy compared with Nutlin, which is overall consistent with the RNA-seq data.